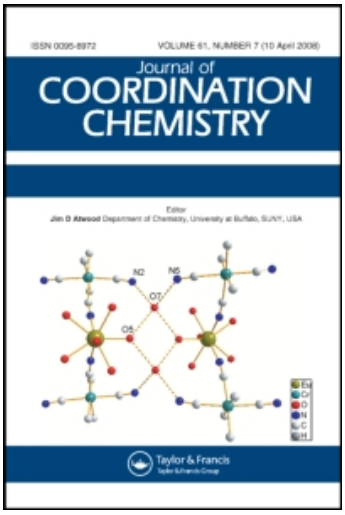

Journal of Coordination Chemistry
Publication details, including instructions for authors and subscription information:
http://www.informaworld.com/smpp/title~content=t713455674

Synthesis and characterization of [$Ru_3(CO)_{12-}$_nL_n] (L = $P(O$ⁱ$Pr)_3$; *n* = 1, 2, 3) and the "Star of David" disorder in bis- and tris-substituted products

Reinout Meijboom[a]; Phibion Dhirori[b]; Ipe J. Mavunkal[b]
[a] Department of Chemistry, University of Johannesburg, Johannesburg, South Africa [b] Department of Chemistry, University of Botswana, Gaborone, Botswana

First published on: 05 October 2009

To cite this Article Meijboom, Reinout , Dhirori, Phibion and Mavunkal, Ipe J.(2010) 'Synthesis and characterization of [$Ru_3(CO)_{12-}$_nL_n] (L = $P(O$ⁱ$Pr)_3$; *n* = 1, 2, 3) and the "Star of David" disorder in bis- and tris-substituted products', Journal of Coordination Chemistry, 63: 1, 79 — 89, First published on: 05 October 2009 (iFirst)
To link to this Article: DOI: 10.1080/00958970903304398
URL: http://dx.doi.org/10.1080/00958970903304398

Journal of Coordination Chemistry
Vol. 63, No. 1, 10 January 2010, 79–89

Taylor & Francis
Taylor & Francis Group

Synthesis and characterization of $[Ru_3(CO)_{12-n}L_n]$ ($L = P(O^iPr)_3$; $n = 1, 2, 3$) and the "Star of David" disorder in bis- and tris-substituted products§

REINOUT MEIJBOOM*†, PHIBION DHIRORI‡ and IPE J. MAVUNKAL*‡

‡Department of Chemistry, University of Johannesburg,
P.O. Box 524, Auckland Park 2006, Johannesburg, South Africa
§Department of Chemistry, University of Botswana,
P. Bag 0704, Gaborone, Botswana

(*Received 8 June 2009; in final form 16 July 2009*)

Disorder in the X-ray structures of $[Ru_3(CO)_{10}\{P(O^iPr)_3\}_2]$ (**3**) and $[Ru_3(CO)_9\{P(O^iPr)_3\}_3]$ (**4**) has been examined. Both structures show a "Star of David" disorder of the Ru_3 triangle. The amount of disorder on the Ru_3 triangle is temperature dependent, where the ligands hardly move, indicating that the whole cluster does not rotate intact in the crystal lattice but rather the Ru_3 triangle effectively oscillates within a relatively rigid ligand polyhedron. The space-group of **4** at 273 K is *P2(1)/n* changing to *P2(1)* upon cooling to 100 K.

Keywords: Ruthenium; Cluster; X-ray; Dynamic disorder

1. Introduction

The structures and fluxionality of the clusters $[M_3(CO)_{12}]$ (M = Fe, Ru, Os) and their derivatives have been studied in great detail [1]. The solid state dynamic NMR behavior of $[Fe_3(CO)_{12}]$ is particularly interesting [2] and has led to considerable controversy [3].

The metal atom disorder observed in $[Fe_2M(CO)_{12}]$ (M = Ru, Os) as well as $[FeRu_2(CO)_{12}]$ is dynamic [4], implying that the metal triangle rotates about the pseudo-threefold axis relative to the crystal lattice. In these systems, however, a distinction between dynamic disorder of the complete molecule or just the M_3 core cannot be made.

Similar disorder on the metal framework was observed in cases where the ligand polyhedra are less symmetric due to substitution of carbonyl groups by isonitriles,

*Corresponding authors. Email: rmeijboom@uj.ac.za; mavunkal@mopipi.ub.bw
§This article is dedicated to Professor John R. Moss on occasion of his 65th birthday.

Journal of Coordination Chemistry
ISSN 0095-8972 print/ISSN 1029-0389 online
DOI: 10.1080/00958970903304398

phosphines, and phosphites [5]. These complexes show a "Star of David" disorder in the metal triangle framework at room temperature X-ray structures. Later, it was shown by X-ray crystallography that the disorder in $[Ru_3(CO)_{11}(CN^tBu)]$, $[Ru_3(CO)_{11}(PMe_3)]$, and $[Ru_3(CO)_9\{P(OMe)_3\}_3]$ is indeed dynamic [6]. It was concluded that the behavior implies that the metal triangle effectively oscillates about the pseudo-threefold axis of the triangle within a relatively rigid ligand polytope.

Here we report our results on the synthesis and characterization of $[Ru_3(CO)_{11}\{P(O^iPr)_3\}]$ (**2**) $[Ru_3(CO)_{10}\{P(O^iPr)_3\}_2]$ (**3**) and $[Ru_3(CO)_9\{P(O^iPr)_3\}_3]$ (**4**) and structural investigation of the triruthenium clusters, **3** and **4**. Dynamic disorder on **4** was observed and upon cooling from 273 to 100 K, a change in the space-group from *P2(1)/n* to *P2(1)* was observed.

2. Experimental

2.1. *General remarks*

All syntheses of air and moisture sensitive compounds were performed using standard Schlenk techniques under pre-purified N_2 [7]. Dichloromethane was pre-dried by passage over alumina (neutral, Brockmann grade I) and subsequently distilled from CaH_2 [8]. $[Ru_3(CO)_{12}]$ (Strem) and $P(O^iPr)_3$ (Aldrich, USA) were used as received.

NMR spectra were recorded on a Bruker Avance 300 MHz spectrometer (^1H : 300 MHz, ^{13}C : 75.5 MHz, ^{31}P : 121.46 MHz) at ambient temperature, and referenced relative to TMS (^1H and ^{13}C) or 85% H_3PO_4 (^{31}P), using the residual protonated impurities in the solvent (^1H NMR : $CDCl_3$: δ 7.27) or external 85% H_3PO_4 (^{31}P). Infrared spectra were recorded in solution cells of sodium chloride windows (optical path length 0.1 mm) on a Perkin–Elmer 2000 FTIR spectrometer. Mass spectrometric analyses were carried out on a Finnigan LCQ Deca spectrometer. Elemental analyses were performed on a Vario Elemental Analyzer.

2.2. *Reaction of $[Ru_3(CO)_{12}]$ (1) with $P(O^iPr)_3$*

To a solution of $[Ru_3(CO)_{12}]$ (**1**) (0.10 g, 0.16 mmol) in dichloromethane (50 cm^3) was added $P(O^iC_3H_7)_3$ (0.1 cm^3, 0.41 mmol), and the resulting mixture was heated under reflux for 3.5 h. The color of the solution changed from orange-yellow to brick-red during this time. The reaction mixture was monitored by TLC and three new products were detected. The volatiles were removed *in vacuo* and the residue taken up in hexane, filtered, and chromatographed on a short silica gel column (8 cm × 2 cm). Unreacted **1** was eluted with hexane and the following three fractions were collected by gradually increasing the polarity of the eluting solvent. The first orange red fraction was collected by 5% CH_2Cl_2 in hexane and was identified as the monosubstituted compound **2**. After evaporation of the solvent, **2** was obtained as a dark-yellow solid (0.002 g; 2%); ν_{CO} cm^{-1} 2066 (s), 1995 (s), 1965 (vs, br), 1952 (sh), 1945 (vs, br); δ_H (300 MHz, $CDCl_3$) 4.68 (m), 1.32 (d) (^3J(HH) 6.18 Hz); $\delta_{C\{H\}}$ (75.5 MHz, $CDCl_3$) 203.9 (–CO), 203.8 (–CO), 71.2 (CH), 23.6 (CH_3); $\delta_{P\{H\}}$ (121.46 MHz, $CDCl_3$) 148; *m/z* (ES) 824 ($M^+ + 2H$) (at least three clear peaks corresponding to CO losses were also observed).

The second fraction was also eluted using 5% CH_2Cl_2 in hexane and identified as the bis-substituted compound **3**. After evaporation of solvent, **3** was obtained as a red solid (0.013 g; 8%); m.p. 148°C; (Found: C 33.4, H 4.5. $Ru_3C_{28}O_{16}P_2H_{42}$ requires C 33.64, H 4.23%); $\nu_{CO}\,cm^{-1}$ 2078 (w), 2023 (s), 2000 (vs, br), 1970 (m, br); δ_H (300 MHz, $CDCl_3$) 4.63 (m), 1.33 (d) (^3J(HH) 6.12 Hz); $\delta_{C\{H\}}$ (75.5 MHz, $CDCl_3$) 70.2 (t, CH), 23.9 (CH_3); $\delta_{P\{H\}}$ (121.46 MHz, $CDCl_3$) 132; *m*/*z* (ES) 1085 ($M^+ + CH_2Cl_2$) (at least four clear peaks corresponding to CO loss were also observed).

The third fraction was eluted using 10% CH_2Cl_2 in hexane and was identified as the tris-substituted compound **4**. After evaporation of the solvent, **4** was obtained as a red solid (0.056 g; 30%); m.p. 142 C; (Found: C 35.00, H 5.62. $Ru_3C_{37}O_{18}P_3H_{65}Cl_2$ (**4** · CH_2Cl_2) requires C 35.13, H 5.18%); $\nu_{CO}\,cm^{-1}$ 2064 (w), 1983 (s, vbr), 1955 (s, br); δ_H (300 MHz, $CDCl_3$) 4.63 (m), 1.32 (d) (^3J(HH) 6.09 Hz); $\delta_{C\{H\}}$ (75.5 MHz, $CDCl_3$) 69.4 (d, CH), 24.0 (d, CH_3); $\delta_{P\{H\}}$ (121.46 MHz, $CDCl_3$) 137; *m*/*z* (ES) 1155 ($M^+ - CO$).

2.3. *Structure determination*

Crystals of **3** were grown from hexane at −4°C. Crystals of **4** were grown from hexane/dichloromethane mixture at −4°C. Single crystal X-ray diffraction data for **3** and **4** were collected on a Bruker X8 Apex II 4K Kappa CCD diffractometer using Mo-Kα (0.71073 Å) radiation with φ-scans at 100(2) K for **3** and φ- and ω-scans at 100(2) K (**4a**) and 273(2) K (**4b**). The initial unit cell and data collection were achieved by the Apex2 [9] software utilizing COSMO [10] for optimum collection of more than a hemisphere of reciprocal space. All reflections were merged and integrated using SAINT [11] and were corrected for Lorentz, polarization and absorption effects using SADABS [11]. The structures were solved by direct method using SIR97 [12] and refined through full-matrix least-squares cycles using SHELX97 [13] with $\Sigma(|F_o| - |F_c|)^2$ being minimized. All nonhydrogen atoms were refined with anisotropic displacement parameters.

Methyl and methine hydrogens were placed in geometrically idealized positions (C–H = 0.98 Å for Me; 1.00 Å for CH) and constrained to ride on their parent atoms, with $U_{iso}(H) = 1.5U_{eq}(C)$ for methyl H atoms and $1.2U_{eq}(C)$ for methine. The deepest residual electron-density hole for **3** (−1.46 e Å^{-3}) is located at 0.05 Å from C252 and the highest peak (1.59 e Å^{-3}) at 0.05 Å from C25. The disorder on the Ru_3 triangle in **3** was refined as 99.2/0.8.

The deepest residual electron-density hole for **4a** (−1.14 e Å^{-3}) is located at 0.05 Å from C462 and the highest peak (1.66 e Å^{-3}) at 1.00 Å from O54. The structure was refined using a twinned refinement. Some thermal motion was observed resulting in large thermal ellipsoids, but these could not be refined using a disordered model. The methyls on *iso*-propyl 35 were refined as a 55.5/44.5 disorder. The disorders on the Ru_3 triangle in **4a** were refined as 91.6/8.4 and 91.3/8.7 disorders, respectively.

The deepest residual electron-density hole for **4b** (−0.81 e Å^{-3}) is located at 0.42 Å from C151 and the highest peak (1.10 e Å^{-3}) at 0.09 Å from C15. Some thermal motion was observed resulting in large thermal ellipsoids, but these could not be refined using a disordered model. The disorder on the Ru_3 triangle in **4b** was refined as 92.6/7.4.

The DIAMOND [14] Visual Crystal Structure Information System software was used for the graphics. Crystal data and details of data collection and refinement are given in table 1.

Table 1. Crystal data and structural refinement for **3**, **4a**, and **4b**.

	3	**4a**	**4b**
Empirical formula	$C_{28}H_{42}O_{16}P_2Ru_3$	$C_{72}H_{125}O_{36}P_6Ru_6$	$C_{36}H_{63}O_{18}P_3Ru_3$
Formula weight	999.77	2358.96	1179.98
Temperature (K)	100(2)	100(2)	273(2)
Wavelength (Å)	0.71073	0.71069	0.71073
Crystal system	Monoclinic	Monoclinic	Monoclinic
Space group	*P2(1)/c*	*P2(1)*	*P2(1)/n*
Unit cell dimensions (Å, °)			
a	15.4235(6)°	9.8081(2)°	9.9425(2)°
b	15.8019(6)°	40.6627(9)°	41.415(1)°
c	17.5614(6)°	13.4459(3)°	13.5542(4)°
α	90	90	90
β	112.4010(10)	110.439(1)	108.686(1)
γ	90	90	90
Volume (Å^3), *Z*	3957.1(3), 4	5024.9(2), 2	5287.0(2), 4
Calculated density (mg m^{-3})	1.678	1.559	1.482
Absorption coefficient (mm^{-1})	1.274	1.050	0.998
F(000)	2000	2398	2400
Crystal size (mm^3)	0.40 × 0.30 × 0.30	0.20 × 0.09 × 0.05	0.25 × 0.09 × 0.06
θ range for data collection (°)	1.43–28.32	1.90–28.36	0.98–28.32
Index ranges	$-19 \le h \le 20$	$-12 \le h \le 13$	$-13 \le h \le 7$
	$-21 \le k \le 19$	$-51 \le k \le 54$	$-55 \le k \le 54$
	$-23 \le l \le 23$	$-17 \le l \le 17$	$-17 \le l \le 18$
Reflections collected	36094	31900	44247
Independent reflections	9848 [R_{int} 0.0263]	21298 [R_{int} 0.0496]	12724 [R_{int} 0.0602]
Completeness to $\theta = 28.32$ (%)	99.7	98.8	96.6
Absorption correction	Semi-empirical from equivalents	Semi-empirical from equivalents	Semi-empirical from equivalents
Max. and min. transmission	0.7010 and 0.6296	0.9494 and 0.8175	0.9426 and 0.7885
Refinement method	Full-matrix least-squares on F^2	Full-matrix least-squares on F^2	Full-matrix least-squares on F^2
Data/restraints/parameters	9848/0/458	21298/5/1093	12724/0/515
Goodness-of-fit on F^2	1.046	1.022	1.024
Final *R* indices [$I > 2\sigma(I)$]	$R_1 = 0.0223$, $wR_2 = 0.0490$	$R_1 = 0.0601$, $wR_2 = 0.1285$	$R_1 = 0.0623$, $wR_2 = 0.1447$
R indices (all data)	$R_1 = 0.0270$, $wR_2 = .0518$	$R_1 = 0.0830$, $wR_2 = 0.1411$	$R_1 = 0.1205$, $wR_2 = 0.1769$
Largest difference peak and hole (e Å^{-3})	1.591 and −1.458	1.665 and −1.138	1.099 and −0.809

3. Results and discussion

3.1. *Synthesis and spectroscopy*

The substitution of carbonyl groups in $[Ru_3(CO)_{12}]$ (**1**) is conveniently achieved by direct reaction when heating the parent compound with appropriate ligands (phosphines, phosphites, etc.) under reflux in solvents such as dichloromethane. Numerous substituted triruthenium complexes have been synthesized using this method [15]. Reaction of an excess of tri-isopropylphosphite with **1**, in dichloromethane, and refluxing, produced mono-, bis-, and tris-substituted products (scheme 1). The compounds **2**, **3**, and **4** were isolated as yellow-red solids using conventional chromatography. The different fractions collected were characterized by spectroscopic methods as well as by elemental analyses.

The IR spectra of the three fractions show bands that can be assigned to terminal CO groups. The IR patterns of these fractions are comparable to that observed for similar mono-, bis-, and tris-substituted triruthenium complexes [16]. As expected, a shift to lower frequency is seen compared to IR of earlier reported mono- and bis-substituted complexes with tris(2,4-di-*tert*-butylphenyl)phosphite (**5**) [17]. The IR patterns of all three fractions are in accord with equatorial substitution of the phosphite ligands.

The proton NMR spectra of the three compounds are similar to the free ligand, showing resonances around δ 4.63 for the methine proton and δ 1.32 for the methyl protons. The two sets of resonances are slightly shifted downfield compared to free ligand around δ 4.37 and δ 1.23. In ^{13}C NMR the methine carbon shifts downfield while the methyl carbons are hardly perturbed upon coordination. Both the mono- and tris-substituted compounds show doublets at δ 71.2 and δ 69.4 with 3.7 and 6.0 Hz, respectively, due to phosphorus coupling. The resonance for the same carbon atom in the bis-substituted compound is a triplet at δ 70.2 with a coupling constant of 3.1 Hz, attributed to virtual coupling of the methine carbon by two phosphorus atoms. The methyl carbons of **2** and **4** are also doublets with a coupling constant of roughly 4 Hz, whereas the similar carbon in **3** appears as a (relatively) broad signal (the three-bond coupling in this case is not well resolved). The carbonyl carbons are not well resolved, but appear around δ 203 in the $^{13}C\{H\}$ NMR.

A single resonance at δ 148 in the $^{31}P\{H\}$ NMR spectrum supports formulation of **2** as the mono-substituted product. The mass spectrum of **2** confirms the molecular formula suggested for **2** with a molecular ion peak around $m/z = 824$ ($M^+ + 2H$), along with peaks corresponding to the loss of carbonyl groups. No meaningful elemental analysis could be performed on this compound as we found portions of it to disproportionate in solution, forming small amounts of bis- as well as tris-substituted products along with some decomposition.

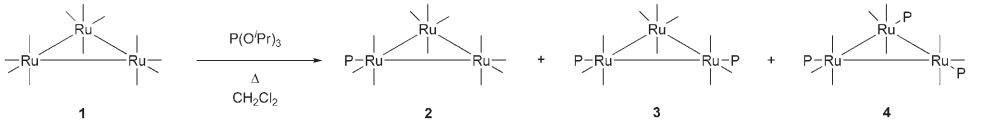

Scheme 1. Synthesis of tri-isopropyl phosphite substituted triruthenium.

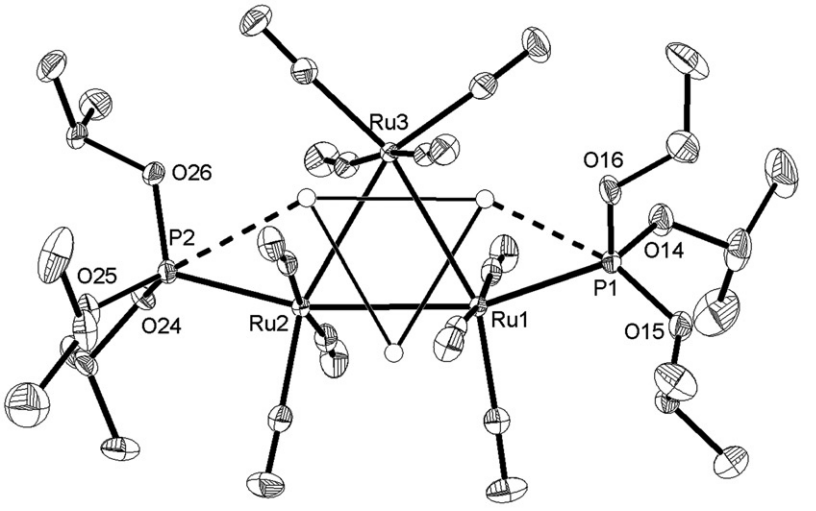

Figure 1. Molecular diagram showing the numbering scheme and displacement ellipsoids (50% probability) of **3**.

The second fraction also showed only one resonance in the $^{31}P\{H\}$ NMR spectrum at δ 132, indicating that both phosphite ligands are in the same chemical environment. We conclude that both phosphites are equatorial *trans* with respect to the phosphite-substituted ruthenium. Unlike the bulky phosphite ligand **5**, which forms various isomers with both $[Ru_3(CO)_{12}]$ and $[Os_3(CO)_{12}]$ for the bis-substituted product, no isomers are observed in the NMR spectra (^1H, $^{13}C\{H\}$ and $^{31}P\{H\}$) of **3** recorded at ambient temperature. The mass spectrum of **3** showed peaks that can be assigned as $M^+ +$ solvent (CH_2Cl_2), as well as peaks that can be ascribed to subsequent carbonyl losses. Satisfactory elemental analysis adds support to the formulation of **3** as the bis-substituted product.

The third, red, fraction also showed only one resonance, at δ 137, in the $^{31}P\{H\}$ NMR spectrum, indicating that all three phosphites are in the same chemical environment. We propose all three phosphite ligands in an equatorial position. Even though the molecular ion peak could not be observed in mass spectra, several peaks attributed to subsequent loss of carbonyl groups can be observed. Elemental analysis shows the inclusion of a molecule of CH_2Cl_2 and provides support for the molecular formula of **4**.

The spectroscopic data of **2**, **3**, and **4** provide sufficient evidence to confirm the products isolated in the reaction are mono-, bis- and tris-substituted compounds $[Ru_3(CO)_{12-n}\{P(O^iPr)_3\}_n]$ ($n = 1, 2, 3$). In addition, we performed single crystal X-ray diffraction studies to unequivocally establish the molecular structures of **3** and **4**.

3.2. *Solid state structures*

A molecular diagram showing the numbering scheme of **3** is presented in figure 1, with selected bond lengths, angles and torsion angles in table 2. Compound **3** crystallizes in the monoclinic space group *P2(1)/c* with $Z = 4$.

Table 2. Selected bond distances (Å) and angles (°) for **3**.

Ru(1)–Ru(2)	2.8418(2)	Ru(1)–P(1)	2.2880(5)
Ru(1)–Ru(3)	2.8444(2)	Ru(2)–P(2)	2.2895(5)
Ru(2)–Ru(3)	2.8558(2)	P(1)–Ru(1A)	2.278(19)
		P(2)–Ru(2A)	2.586(19)
Ru(1)–Ru(2)–Ru(3)	59.897(5)	P(1)–Ru(1)–Ru(2)	159.088(14)
		P(2)–Ru(2)–Ru(1)	159.173(15)

The structure of **3** represents a triangular ruthenium cluster with the two phosphite ligands in equatorial *trans–trans* orientation with respect to the phosphite-substituted ruthenium. The almost exclusive tendency for P-donor ligands to occupy an equatorial site with respect to the triruthenium plane was noted previously [5].

The structure of **3** shows a "Star of David" disorder on the Ru_3 triangle, and Ru–P distances of both the major and the minor component of the disorder are approximately the same at 2.28 Å (table 2). The carbonyl ligands are slightly bent to accommodate the two different disordered components of the Ru_3 triangle.

The determination of the X-ray structure of one of the molecules of **4** at 100 K is depicted in figure 2 with selected bond lengths and angles in table 3. Compound **4** crystallizes in the monoclinic space group *P2(1)* with $Z = 2$ when recorded at 100 K. The structure of **4** also represents a triangular ruthenium cluster with the phosphite ligands equatorial.

The determination of the X-ray structure of **4** at 100 K also shows a "Star of David" disorder on the Ru_3 triangle. This structure shows two independent molecules in the asymmetric unit of the monoclinic space group *P2(1)*. When the same structure was determined at 273 K, the two independent units collapsed to one independent molecule with an additional symmetry element in the unit cell, resulting in the space-group being *P2(1)/n* ($Z = 4$) as well as all distances, and the disorder, averaged (table 3).

It was previously observed that di- and tri-substituted triruthenium clusters, such as **3** and **4**, are able to support a dynamic "Star of David" disorder due to the similarity of the ligand polytope [5, 6]. In these systems, the periphery of the molecule is so similar to that of its inversion image that it is capable of accommodating two possible dispositions of the Ru_3 core, given that the distortions in the core environment are such that two isomers with very similar ligand arrays are feasible. Such a situation is compatible with the fluxional nature of many of these systems in solution. In figure 3(a) an overlap of the two independent molecules of **4a** is presented, with one of them inverted. It shows that the differences between the two independent units are marginal and that they can be related through an inversion center at higher temperatures. Figure 3(b) shows the overlap of the two independent units (P atoms overlapping), showing clearly that the coordination polytope, formed by carbonyl oxygens and phosphorus, marginally changes upon inversion of the Ru_3 core. This observation supports the possibility of a dynamic disorder of the Ru_3 core in these systems.

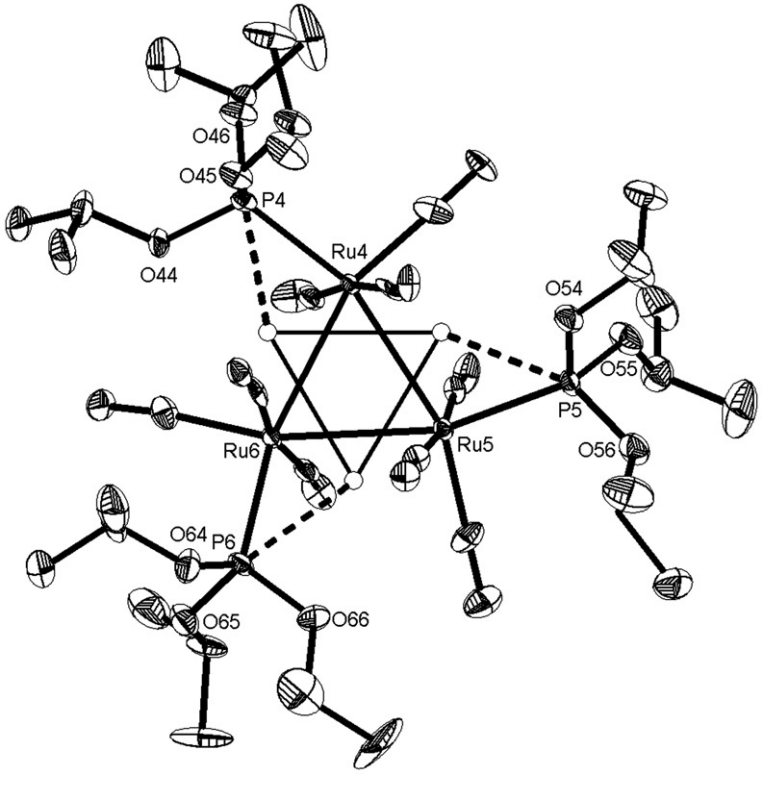

Figure 2. Molecular diagram showing the numbering scheme and displacement ellipsoids (50% probability) of one of the independent molecules of **4a** at 100 K.

Table 3. Selected bond distances (Å) and angles (°) for **4a** and **4b**.

4a			
Ru(1)–Ru(2)	2.8498(12)	Ru(1)–P(1)	2.302(2)
Ru(1)–Ru(3)	2.8544(12)	Ru(2)–P(2)	2.292(2)
Ru(2)–Ru(3)	2.8481(14)	Ru(3)–P(3)	2.286(2)
Ru(4)–Ru(5)	2.8556(12)	Ru(4)–P(4)	2.301(2)
Ru(4)–Ru(6)	2.8618(12)	Ru(5)–P(5)	2.302(2)
Ru(5)–Ru(6)	2.8497(13)	Ru(6)–P(6)	2.284(2)
4b			
Ru(1)–Ru(2)	2.8610(7)	Ru(1)–P(1)	2.2818(16)
Ru(1)–Ru(3)	2.8498(7)	Ru(2)–P(2)	2.2928(18)
Ru(2)–Ru(3)	2.8487(8)	Ru(3)–P(3)	2.2872(19)
4a			
Ru(1)–Ru(2)–Ru(3)	60.13(3)	P(1)–Ru(1)–Ru(2)	156.18(6)
Ru(2)–Ru(3)–Ru(1)	59.97(3)	P(2)–Ru(2)–Ru(1)	102.78(7)
		P(3)–Ru(3)–Ru(1)	156.65(7)
Ru(4)–Ru(5)–Ru(6)	60.21(2)	P(4)–Ru(4)–Ru(5)	155.98(6)
Ru(5)–Ru(6)–Ru(4)	60.00(3)	P(5)–Ru(5)–Ru(4)	101.97(7)
		P(6)–Ru(6)–Ru(4)	153.75(6)
4b			
Ru(1)–Ru(2)–Ru(3)	59.884(18)	P(1)–Ru(1)–Ru(2)	103.77(5)
Ru(2)–Ru(3)–Ru(1)	60.273(18)	P(2)–Ru(2)–Ru(1)	156.22(5)
		P(3)–Ru(3)–Ru(1)	102.76(5)

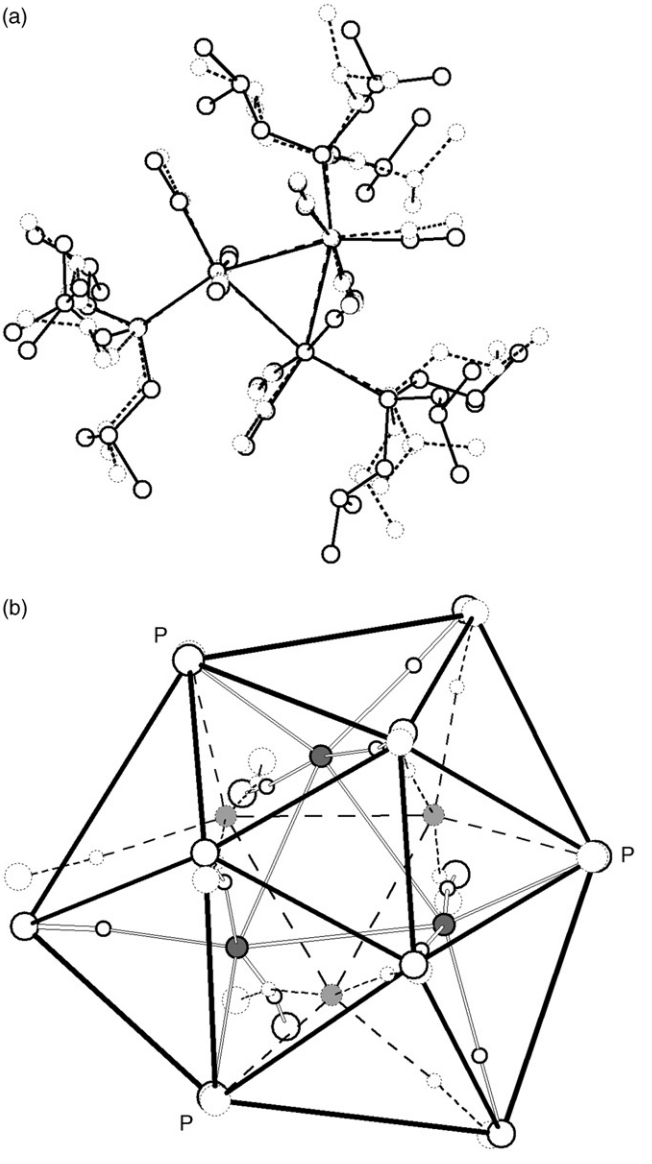

Figure 3. (a) Overlay of the two independent molecules of **4a** (molecule 2 – dashed – was inverted) and (b) overlay of the two independent molecules of **4a** showing the coordination polyhedron to be (slightly distorted) icosahedral.

A slight deviation from linearity for the carbonyls was observed in all three structures. However, in contrast with previously reported structures [6], even at room temperature this deviation was deemed too small to describe the carbonyl ligands as semi-bridging.

Weak hydrogen interactions were observed in all three structures and are described in table 4. When investigating the difference between the hydrogen interactions of

Table 4. Selected inter- and intra-molecular hydrogen interactions (Å) and angles (°) for **3**, **4a**, and **4b**.

D–H···A	*d*(D–H)	*d*(H···A)	*d*(D···A)	∠(DHA)
3				
C(14)–H(14) ···O(15)	1.00	2.34	2.775(3)	105.3
4a				
C(142)–H(14d)···O(33)	0.98	2.58	3.417(14)	143.2
C(162)–H(16f)···O(15)	0.98	2.42	3.081(13)	123.9
C(242)–H(24f)···O(26)	0.98	2.48	3.105(13)	121.5
C(261)–H(26c)···O(22)	0.98	2.6	3.284(12)	127.3
C(262)–H(26d)···O(25)	0.98	2.58	3.193(13)	120.5
C(442)–H(44f)···O(45)	0.98	2.51	3.134(11)	121.3
C(451)–H(45c)···O(42)	0.98	2.57	3.267(14)	128.4
C(542)–H(54d)···O(55)	0.98	2.45	3.056(14)	119.9
C(551)–H(55c)···O(56)	0.98	2.6	3.146(13)	115.5
C(662)–H(66d)···O(41)[a]	0.98	2.37	3.332(13)	166.8
C(662)–H(66f)···O(64)	0.98	2.39	3.042(13)	123.7
4b				
C(142)–H(14C) ···O(15)	0.96	2.37	3.059(11)	128.7
C(361)–H(36F) ···O(32)	0.96	2.55	3.417(14)	151.0

Symmetry transformations used to generate equivalent atoms: [a] $x+1$, y, z.

4a and **4b**, the decreased interactions for **4b** are the result of describing the structure as the average of the two units in **4a**.

4. Conclusion

The reaction of $[Ru_3(CO)_{12}]$ with $P(O^iPr)_3$ yielded **2**, **3**, and **4**, which were fully characterized using spectroscopic methods. In addition, the molecular structures of **3** and **4** were determined using X-ray diffraction. Both structures showed a "Star of David" disorder on the Ru_3 triangle. The disorder on **4** was temperature dependent, and consequently dynamic in nature. To the best of our knowledge this is the first example where the tris-substituted triruthenium clusters show a dynamic disorder of the Ru_3 core.

Supplementary material

CCDC 693703 (**3**), 693704 (**4a**) and 693705 (**4b**) contains the supplementary crystallographic data for this article. These data can be obtained free of charge via http://www.ccdc.cam.ac.uk/conts/retrieving.html, or from the Cambridge Crystallographic Data Centre, 12 Union Road, Cambridge CB2 1EZ, UK; Fax: (+44) 1223-336-033; or E-mail: deposit@ccdc.cam.ac.uk.

Acknowledgements

Financial assistance from the Research and Publication Committee, University of Botswana, South African National Research Foundation and the Research Fund of the

University of Johannesburg and SASOL is gratefully acknowledged. Part of this material is based on work supported by the South African National Research Foundation. Opinions, findings, conclusions or recommendations expressed in this material are those of the authors and do not necessarily reflect the views of the NRF.

References

[1] (a) D. Braga, F. Grepioni, L.J. Farrugia, B.F.G. Johnson. *J. Chem. Soc., Dalton Trans.*, 2911 (1994) and references therein; (b) L.J. Farrugia. *J. Chem. Soc., Dalton Trans.*, 1783 (1997).
[2] (a) B.E. Hanson, E.C. Lisic, J.T. Petty, G.A. Iannaconne. *Inorg. Chem.*, **25**, 4062 (1986); (b) S. Aime, R. Gobetto. *J. Cluster Sci.*, **4**, 1 (1993); (c) H. Adams, N.A. Bailey, G.W. Bentley, B.E. Mann. *J. Chem. Soc., Dalton Trans.*, 1831 (1989).
[3] (a) B.E. Mann. *J. Chem. Soc., Dalton Trans.*, 1457 (1997); (b) B.F.G. Johnson. *J. Chem. Soc., Dalton Trans.*, 1473 (1997).
[4] (a) D. Braga, L.J. Farrugia, A.L. Gillon, F. Grepioni, E. Tedesco. *Organometallics*, **15**, 4684 (1996); (b) L.J. Farrugia, A.M. Senior, D. Braga, F. Grepioni, A.G. Orpen, J.G. Crossley. *J. Chem. Soc., Dalton Trans.*, 631 (1996).
[5] (a) M.I. Bruce, M.J. Liddell, C.A. Hughes, B.W. Skelton, A.H. White. *J. Organomet. Chem.*, **347**, 157 (1988); (b) M.I. Bruce, M.J. Liddell, C.A. Hughes, J.M. Patrick, B.W. Skelton, A.H. White. *J. Organomet. Chem.*, **347**, 181 (1988); (c) M.I. Bruce, M.J. Liddell, O. bin Shawkataly, C.A. Hughes, B.W. Skelton, A.H. White. *J. Organomet. Chem.*, **347**, 207 (1988); (d) M.I. Bruce, M.J. Liddell, O. bin Shawkataly, I. Bytheway, B.W. Skelton, A.H. White. *J. Organomet. Chem.*, **369**, 217 (1989); (e) M.I. Bruce, J.G. Matisons, R.C. Wallis, J.M. Patrick, B.W. Skelton, A.H. White. *J. Chem. Soc., Dalton Trans.*, 2365 (1983); (f) M.I. Bruce, G.N. Pain, C.A. Hughes, J.M. Patrick, B.W. Skelton, A.H. White. *J. Organomet. Chem.*, **307**, 343 (1986); (g) M.I. Bruce, B.W. Skelton, A.H. White, N.N. Zaitseva. *Aust. J. Chem.*, **50**, 163 (1997).
[6] L.J. Farrugia, C. Rosenhahn, S. Whitworth. *J. Cluster Sci.*, **4**, 505 (1998).
[7] (a) D.F. Shriver, M.A. Drezdzon. *The Manipulation of Air-Sensitive Compounds*, Wiley-Interscience, New York (1986); (b) R.J. Errington. *Advanced Practical Inorganic and Metalorganic Chemistry*, Blackie Academic, London (1997).
[8] D.D. Perrin, W.L.F. Armarego. *Purification of Laboratory Chemicals*, Pergamon Press, Oxford (1988).
[9] Bruker Advanced X-ray Solutions. *Apex 2 (Version 1.0-27)*, Bruker AXS Inc., Madison, Wisconsin, USA (2005).
[10] Bruker Advanced X-ray Solutions. *COSMO (Version 1.48)*, Bruker AXS Inc., Madison, Wisconsin, USA (2003).
[11] Bruker Advanced X-ray Solutions. *SAINT-PLUS (Version 7.12)*, *XPREP* and *SADABS (Version 2004/1)*, Bruker AXS Inc., Madison, WI, USA.
[12] A. Altomare, M.C. Burla, M. Camalli, G.L. Cascarano, C. Giacovazzo, A. Guagliardi, A.G.G. Moliterni, G. Polidori, R. Spagna. *J. Appl. Cryst.*, **32**, 115 (1999).
[13] G.M. Sheldrick. *SHELXL97, Program for Solving Crystal Structures*, University of Göttingen, Göttingen, Germany (1997).
[14] K. Brandenburg, H. Putz. *DIAMOND, 2005, (Version 3.0c)*, Crystal Impact GbR, Bonn, Germany.
[15] K.H. Whitmire. In *Comprehensive Organometallic Chemistry*, E.W. Abel, F.G.A. Stone, G. Wilkinson (Eds), Vol. 7, 2nd Edn, pp. 343–408, Pergamon Press, Oxford, UK (1995).
[16] N. Begum, M.A. Rahman, M.R. Hasan, D.A. Tocher, E. Nordlander, G. Hogarth, S.E. Kabir. *J. Organomet. Chem.*, **693**, 1645 (2008) and references therein.
[17] A.O. Magwaza, R. Meijboom, A. Muller, I.J. Mavunkal. *Inorg. Chim. Acta*, **361**, 335 (2008).